Published in final edited form as:
NMR Biomed. 2014 October ; 27(10): 1167–1175. doi:10.1002/nbm.3170.

Measurement of regional variation of GABA in the human brain by optimized point-resolved spectroscopy at 7T in vivo

Sandeep K. Ganji[1,2], **Zhongxu An**[1,2], **Abhishek Banerjee**[1], **Akshay Madan**[1], **Keith M. Hulsey**[1,2], and **Changho Choi**[1,2,*]

[1]Advanced Imaging Research Center, University of Texas Southwestern Medical Center, Dallas, Texas, USA

[2]Department of Radiology, University of Texas Southwestern Medical Center, Dallas, Texas, USA

Abstract

The ^{1}H resonances of GABA in the human brain *in vivo* are extensively overlapped with the neighboring abundant resonances of other metabolites and remain indiscernible in short TE MRS at 7T. Here we report the GABA resonance at 2.28 ppm can be fully resolved by means of echo time optimization of a point-resolved spectroscopy (PRESS) scheme. Following numerical simulations and phantom validation, the subecho times of PRESS was optimized at (TE_1, TE_2) = (31, 61) ms for detection of GABA, glutamate (Glu), glutamine (Gln) and glutathione (GSH). The *in-vivo* feasibility of the method was tested in several brain regions in 9 healthy subjects. Spectra were acquired from the medial prefrontal, left frontal, medial occipital and left occipital brain and analyzed with LCModel. Following the gray and white matter (GM and WM) segmentation of T_1-weighted images, linear regression of metabolite estimates was performed against the fractional GM contents. The GABA concentration was estimated to be about 7 fold higher in GM than in WM. GABA was overall higher in frontal than in occipital brain. Glu was ~2 fold higher in GM than in WM in both frontal and occipital brain. Gln was significantly different between frontal GM and WM while being similar between occipital GM and WM. GSH did not show significant dependence on tissue content. The signals from N-acetylaspartylglutamate were clearly resolved, giving the concentration higher by > 10 fold in WM than in GM. Our data indicate that the PRESS TE = 92 ms method provides an effective means for measuring GABA and several challenging J-coupled spin metabolites in human brain at 7T.

Keywords

GABA; Human brain; ^{1}H MRS; 7T; Point-resolved spectroscopy (PRESS); Gray matter; White matter

INTRODUCTION

The *in vivo* measurement of γ-aminobutyric acid (GABA), the primary inhibitory neurotransmitter in the mammalian brain, has considerable potential for the investigation of

*Correspondence to: Changho Choi, PhD, Advanced Imaging Research Center, 5323 Harry Hines Blvd., Dallas, Texas, USA 75390, changho.choi@utsouthwestern.edu.

a wide variety of neuropsychiatric disorders (1). The proton magnetic resonances of GABA are all proximate to the resonances of other abundant metabolites (2) and thus precise measurement of this low-concentration metabolite is challenging. At low or intermediate field strengths, since direct measurement of GABA is very difficult, spectral editing approaches are commonly used to detect GABA. For instance, the 3.01 ppm resonance of GABA can be edited by means of difference editing (3–6) and double-quantum filtering (7,8), utilizing the J coupling of the 3.01 ppm resonance to the resonance at 1.89 ppm. At high fields, spectral resolution of coupled resonances is notably improved (9) because the coupling strength which governs the overall linewidth of the multiplets is independent of field strength while the chemical shift differences (in Hz) increases with field strength. With this enhancement in spectral resolution and signal gain at high fields, several studies reported MRS measures of many brain metabolites, including GABA, using conventional sequence schemes with short echo times at 7T (10–12). Despite the presence of substantial macromolecule (MM) signals (13,14), many small signals were well resolved with good shimming and GABA in medial occipital brain was measured with good precision in these previous studies.

GABA has six non-exchangeable protons from $^{2}CH_2$, $^{3}CH_2$, and $^{4}CH_2$ groups, which resonate at 2.284, 1.888, and 3.012 ppm respectively, with J coupling strengths of 6.4 – 8.1 Hz (5,15). While the C3- and C4-proton signals of GABA are extensively obscured by the large signals of N-acetylaspartate (NAA) and total creatine (tCr), the C2-proton resonance at 2.28 ppm is relatively distant from the neighboring resonance of glutamate (Glu) at 2.35 ppm. The GABA C2 and Glu C4 proton signals, which are 18 Hz apart from each other at 7T, are both triplets with an overall width > 14 Hz, and thus the GABA multiplet appears largely overlapped with the Glu signal in short TE spectra. Since the spectral pattern of J coupled resonances varies with inter-RF (radio frequency) pulse timings, the selectivity of the GABA signal against the Glu resonance can be improved with modification of the sequence timings, with an additional advantage that the MM signals are suppressed at long TE, as demonstrated with STEAM (stimulated echo acquisition mode) in a prior study at 3T (16).

In this paper, we report an intermediate-TE PRESS approach for detection of GABA at 7T. The subecho times are refined, with numerical and phantom analyses, to achieve good selectivity of the GABA 2.28 ppm signal against Glu. Although extensive suppression of Glu may be the most beneficial for GABA detection as in the prior 3T study with STEAM (16), given the clinical significance of Glu, the Glu 2.35 ppm signal is moderately retained for co-detection of GABA and Glu. With the improved GABA detectability, the method is applied to measure GABA, using a volume RF coil, in various brain regions with high or low GABA concentrations in frontal and occipital brain and to evaluate the GABA levels in gray and white matter *via* linear regression analysis of the measures with respect to fractional gray matter contents. Similar analysis is presented for Glu, Gln, GSH and NAAG (N-acetyl-aspartyl-glutamate), together with analysis of NAA, tCr and tCho (total choline).

MATERIALS and METHODS

Numerical density-matrix simulations were carried out to optimize the subecho times of a PRESS sequence to improve the spectral resolution between the GABA 2.28 ppm and Glu 2.35 ppm resonances. 3D-volume localized spectra were calculated for various subecho times, TE_1 and TE_2, incorporating the experimental RF and gradient pulse waveforms, according to a product-operator based transformation-matrix method described in a prior study (17). The simulations were programmed with Matlab (The MathWorks, Inc.). The GABA-optimized PRESS sequence was validated in a phantom solution with GABA (2 mM), Glu (20 mM) and creatine (Cr) (16 mM).

Nine healthy volunteers were enrolled in the study (5 female and 4 male; age 21 – 32, median 24). MR experiments were carried out in a 7T whole-body scanner (Philips Medical Systems), equipped with quadrature birdcage RF transmission and 16-channel signal reception. The protocol was approved by the Institutional Review Board of the University of Texas Southwestern Medical Center. Written informed consent was obtained prior to the scans.

In vivo single-voxel localized ^{1}H MR spectra were obtained, with a GABA-optimized PRESS sequence (TE = 92 ms), from four brain regions in each of the 9 subjects; namely, medial prefrontal, left frontal, medial occipital and left occipital brain. Slice-selective RF pulses included an 8.8-ms 90° RF pulse (bandwidth = 4.7 kHz) and an 11.9-ms 180° RF pulse (bandwidth = 1.4 kHz) at B_1 = 15 μT. PRESS acquisition parameters included TR = 2.5 s, acquisition bandwidth = 5 kHz, and 2048 sampling points. The voxel size ranged from 10 to 15 mL. The number of signal averages (NSA) was 192 – 256, depending on the voxel size and brain regions (256 averages for the scans in left frontal and occipital regions). The carrier frequencies of the slice selective RF pulses were set to 2.5 ppm. An unsuppressed water signal was acquired from each voxel using an RF carrier at the water resonance for residual eddy current compensation. An unsuppressed short-TE (13 ms) water signal was acquired using TR = 2.5 s from the same voxel. 3D sagittal T_1-weighted image was acquired with TR/TE/TI = 2500/3.7/1300 ms, flip angle = 8°, field of view = 240×240 mm, and 150 slices (slice thickness = 1.0 mm). Metabolite T_2 measurement was conducted for the medial occipital brain in a subject, with NSA = 32 at each of 11 TEs (75 – 275 ms; increments of 20 ms) and TR = 2.5 s.

The data from the 16 channels were combined off-line, using an in-house Matlab script which was developed according to a published algorithm (18). The combined data were then zero filled to 8192 points prior to Fourier transformation. Spectral fitting was performed with LCModel software (Ver 6.2) (19), using numerically-calculated basis spectra of 16 metabolites; GABA, Glu, Gln, GSH, NAA, NAAG, tCr (creatine + phosphorouscreatine), tCho (glycerophosphocholine + phosphocholine), myo-inositol, glycine, taurine, scyllo-inositol, aspartate, phosphoethanolamine, ethanolamine, and lactate. Published chemical shift and J coupling constants were used for calculating the basis function; Kaiser *et al*. (5) for GABA, Choi *et al*. (20) for GSH, and Govindaraju *et al*. (2) for other metabolites. The spectral fitting was performed between 0.5 and 4.2 ppm. Cramer-Rao lower bound (CRLB), which is the measure of precision (21), computed from the Cramer-Rao Theorem that uses

the diagonal elements of the least-squares variance-covariance matrix (19), was returned as a percentage standard deviation (SD) by LCModel. The fractions of gray and white matter (GM and WM) and cerebrospinal fluids (CSF) within the MRS voxels were obtained from segmentation of the T_1-weighted images using Statistical Parametric Mapping software (SPM5) (22). The tissue segmentation was undertaken incorporating the chemical shift displacement effect. A major resonance was chosen for each metabolite based on the highest signal selectivity and used to calculate the voxel displacement according to the spectral difference of the resonance from the RF carrier (2.5 ppm). The major resonance used was 2.01, 2.045, 2.28, 2.35, 2.44, 2.54, 3.03 and 3.21 for NAA, NAAG, GABA, Glu, Gln, GSH, tCr and tCho, respectively. The metabolite signal estimates from LCModel were normalized with respect to the water signal from GM and WM. Metabolite concentrations were then calculated by setting the mean value of the tCr estimates from the medial occipital brain at 8 mM (10,11). The T_2 relaxation effect on the metabolite signal was corrected using experimental T_2 values obtained within the study. To obtain the metabolite concentrations in pure GM and WM, the metabolite estimates from the brain regions were fitted with a linear function of fractional GM matter content, f_{GM} = GM/(GM+WM). Prism 5 (GraphPad Software, Inc.) was used for the linear regression and relevant statistical analyses. Paired t-test was performed for comparison of metabolite estimates and regression outputs between brain regions. Statistical significance was declared at p value < 0.05. Data are presented in mean±SD.

RESULTS

We performed numerical simulations and obtained a PRESS subecho time set (TE_1, TE_2) = (31, 61) ms for detection of GABA and Glu at 7T, where TE_1 and TE_2 are the subecho times of the first and second slice-selective 180° RF pulses respectively. At this PRESS TE = 92 ms, the GABA and Glu multiplets between 2.2 and 2.4 ppm were narrow and completely separated up to singlet linewidth (FWHM) of 14 Hz, as indicated by simulation results in Fig. 1a. The overall widths of the GABA 2.28 ppm and Glu 2.35 ppm multiplets were smaller by ~2 fold compared to 90°-acquisition for potential *in-vivo* singlet FWHM of 8 – 12 Hz. Of note, the multiplet widths at TE = 92 ms were comparable to singlet linewidth; for instance, for singlet FWHM of 10 Hz, the GABA and Glu multiplet widths were 10 –10.5 Hz at the level of (positive amplitude + negative amplitude)/2, whilst the GABA and Glu multiplet widths of 90°-acquisition were 18.5 – 19 Hz. Ignoring T_2 relaxation effects, the signal strengths of GABA and Glu were 72% and 58% with respect to the 90°-acquisition. As a result, when the GABA and Glu multiplets were summed for a GABA-to-Glu concentration ratio of 1:10, the GABA 2.28 ppm signal, which was not discernible in 90°-acquisition for singlet FWHM > 8 Hz, became clearly differentiable from Glu at PRESS TE = 92 ms. For the same concentration ratio, the calculated composite signal pattern of PRESS TE = 92 ms was closely reproduced in phantom experiment (Fig. 1b). The zero-TE calculated composite signals of GABA and Glu were very similar to phantom spectra obtained with STEAM (TE, TM) = (8, 14) ms, in which the J evolution effects may be negligible.

T_2 relaxation times of Glu, NAA, tCr and tCho in the medial occipital brain were measured for use to correct for the transverse relaxation effects. The singlets of NAA, tCr and tCho at

TE = 275 ms were 26%, 15% and 23% relative to those at TE = 75 ms, respectively (Fig. 2a). With increasing TE, the intensity and pattern of the Glu multiplet at 2.35 ppm were both altered due to the T_2 relaxation and J coupling effects. The Glu signal was relatively well defined at TE = 75 – 115 ms and 215 – 255 ms. From mono-exponential fitting of the LCModel estimates of the signals as a function of TE, the T_2's of Glu, NAA, tCr and tCho were estimated to be 121, 147, 106 and 141 ms, respectively. The T_2 estimates of NAA and tCr agreed well with prior measures by PRESS at 7T (23). The T_2 values of Glu, NAA, tCr and tCho were used for subsequent data analysis for metabolite quantification. The T_2's of GABA, Gln and GSH were assumed to be identical to the Glu T_2.

Figure 3 presents *in-vivo* spectra from the medial frontal (MF) and left frontal (LF) brain of a healthy volunteer, together with spectral analysis results. The fractional GM content was 78% and 18%, respectively. With the substantial attenuation of MM signals at TE = 92 ms, the spectra had fairly flat baselines and were well reproduced by the fit with minimal variations in residuals between 0.5 and 4.2 ppm (Fig. 3b). As predicted by the simulation and phantom data, the GABA signal at 2.28 ppm was resolved from the large Glu 2.35 ppm peak (Fig. 3c). The GABA signal was clearly discernible in the spectrum from the MF voxel (GM dominant), whilst the spectrum from the WM-rich, LF region showed a small signal at 2.28 ppm. The GABA concentration estimate was higher by > 2 fold in GM- than in WM-dominant regions. The GABA CRLB was 5% and 9% in spectra from GM and WM regions, respectively. The Glu signal at 2.35 ppm was also greater in GM- than in WM-dominant region. The Glu CRLB was 1 – 2% in both spectra. The spectrum from the LF showed a small Gln signal at 2.44 ppm compared to the MF spectrum. The NAAG singlet at 2.045 ppm was unequivocally discernible in the spectrum from LF, indicating higher NAAG in WM than in GM. The 2.18 ppm multiplet of the NAAG glutamate moiety was also larger in LF than in MF.

For validation of GABA detection, LCModel fitting was undertaken with and without GABA in the basis set. In the spectral fitting with GABA, the *in vivo* spectra were well reproduced by the fits, leading to noise-level residuals at GABA resonances (Fig. 3c, Residuals-1). When GABA was excluded from the basis set, large residuals at the GABA 2.28 and 1.89 ppm resonances resulted (Fig. 3c, Residuals-2), supporting that the signals at 2.28 and 1.89 ppm in the *in-vivo* spectra were primarily attributable to GABA. The residuals from without-GABA fitting were larger in spectra from GM regions than in spectra from WM regions.

The signal-to-noise ratio (SNR) and linewidth were quite similar between the 36 data sets from 9 subjects (4 voxels in each). For spectra from the MF, LF, MO (medial occipital), and LO (left occipital) regions, the mean SNR of NAA (2.01 ppm) was 304±37, 296±25, 313±36 and 302±37, and the mean linewidth of tCr (3.03 ppm) was 10.1±0.9, 9.2±0.7, 9.6±0.6 and 9.9±0.8, respectively. Here, the SNR was the ratio of the tNAA singlet amplitude with respect to the SD of the residuals between 1.7 and 3.3 ppm. As shown in Table 1, the fractional GM content was approximately 70% for the voxels in the MF and MO regions and about 20% for the voxels in the LF and LO regions.

GABA was measurable with CRLB < 16% in all 36 spectra. The concentration of GABA was estimated to be 1.0±0.1, 0.4±0.1, 0.8±0.1, and 0.3±0.1 mM for the MF, LF, MO and LO regions, respectively (Table 1). The estimate was significantly different between MF and LF and between MO and LO ($p < 2\times10^{-6}$). Also, the GABA estimate was significantly different between MF and MO regions ($p = 9\times10^{-4}$) while the f_{GM} was about the same between the regions (p = 0.5). Linear regression of the GABA estimates with respect to f_{GM} showed slightly stronger correlation of the concentration with f_{GM} in frontal brain than in occipital brain (slope = 1.1 *vs*. 0.9), but the difference in the slopes was not significant (p = 0.06) (Fig. 4). The GABA level in pure GM (*i.e.*, Y-axis intercept at $f_{GM} = 1$) was estimated to be 1.3 and 1.0 mM for frontal and occipital brain respectively, which were significantly different from each other (p = 0.001). The GABA concentration in pure WM (*i.e.*, Y-axis intercept at $f_{GM} = 0$) was about the same between frontal and occipital brain (~0.15 mM). The ratio of the Y-axis intercepts was 7.5±2.7 and 7.5±2.9 for frontal and occipital brain, respectively. The GABA CRLB ranged from 4% to 7% in the data from the MF and MO regions, while it was relatively large (8 – 16%) in the data from the LF and LO regions.

The Glu estimate was significantly different between the MF and LF regions and between the MO and LO regions ($p < 2\times10^{-6}$) (Table 1). Linear regression showed that the correlation of Glu with f_{GM} was about the same between frontal and occipital brain (slope = 6.4). Glu showed significant difference between MF and MO regions and between LF and LO regions (p < 0.02) (Fig. 5). The Glu CRLB was ≤2% in all data. For Gln, the GM and WM dependence of the estimate was markedly different between frontal and occipital brain. While the mean Gln level was similar between the MO and LO regions (~2.3 mM), the data from the MF and LF regions showed drastically different Gln levels (1.5 and 0.4 mM respectively; $p = 3\times10^{-5}$), giving a correlation slope of 2.0, which was significantly different from the (essentially) zero slope in the occipital-brain data ($p = 1^{-9}$). The Gln difference between MF and LF remained significant ($p = 2.4\times10^{-4}$) following a Bonferroni correction, which was done by multiplying the uncorrected p value by the number of metabolites, 8. The Gln CRLB of the LF region was distinctly larger than those of other regions (9 – 31% *vs*. 2 – 6%). For GSH, the concentration was estimated to be more or less 1 mM in the four regions. The estimates from the MF and MO were significantly different from each other (1.1 and 0.8 mM respectively; p = 0.01). Linear regression analysis suggested that the GSH concentration may be higher in frontal GM than in occipital GM (p = 0.02). In contrast to many other metabolites, NAAG showed negative correlation with f_{GM}. The NAAG estimate was very similar between frontal and occipital brain. The mean concentration of the LF and LO regions was ~2.5 times higher than that of the MF and MO regions (1.9 *vs*. 0.8 mM). A linear regression of the entire 36 estimates of NAAG gave the ratio of the Y-axis intercepts at $f_{GM} = 0$ and 1 as 33±42. The concentration of NAA was estimated to be fairly constant between the four regions (9 – 10 mM), without an indication of significant difference between GM and WM or between frontal and occipital brain. For tCho, the concentration from the MF region was distinctly larger than those from other regions (1.9 *vs*. ~1.3 mM) (Table 1). The concentration was significantly different between GM- and WM-dominant regions ($p = 6\times10^{-5}$ in frontal and 0.01 in occipital). The correlation with f_{GM} was quite different between frontal and occipital brain, the slope being positive (0.9) in frontal brain and negative (−0.4) in occipital brain, which were both significantly different from zero (p =

4×10^{-8} and 0.01 respectively). The tCr estimates from the MF, LF, MO, and LO regions were 8.6, 5.4, 8, and 6.4 mM, respectively. The tCr level was significantly different between GM- and WM-rich regions ($p < 4\times10^{-6}$). The GM tCr levels in frontal and occipital brain (10.0 and 8.9 mM respectively) were significantly different from each other ($p = 0.02$).

DISCUSSION

Although, at 7T, short-TE MRS gives large signals with minimal T_2 signal loss, the spectral overlaps between the broad multiplets and interference of MM signals could make GABA estimation from short-TE data difficult, as in our prior study (20). Given the spectral complexities at short TEs, simplification of spectra *via* suppression of MM signals and manipulation of the J evolution at an optimized intermediate TE can provide an alternative tool for measuring small metabolite signals. The current paper reports regional variations of GABA, Glu, Gln, GSH and NAAG, together with those of NAA, tCho and tCr, using PRESS (TE_1, TE_2) = (31, 61) ms, which was tailored for improving the spectral resolution of the J coupled resonances between 2.1 and 2.6 ppm, particularly for GABA. This PRESS TE = 92 ms method gave substantial narrowing of the GABA 2.28 ppm and Glu 2.35 ppm multiplets and allowed improved differentiation of the small GABA signal from the adjacent Glu peak compared to our previously-reported TE = 100 ms method (20). The Glu signal amplitude was slightly suppressed to increase the GABA selectivity, but this is not detrimental to Glu detection given the overall small CRLB of Glu in the present study (2% or less). In particular, acquisition of *in-vivo* data that show a visually discernible GABA peak at 2.28 ppm may be a major achievement of the present study. The GABA CRLB was reduced compared to our prior study (*i.e.*, ~5% *vs.* ~15% for medial frontal brain), indicating improved precision. Additionally, spectral fitting without GABA resulted in noticeable residuals at the GABA resonances, indicating good selectivity of GABA by the optimized MRS. In addition, it is noteworthy that the GABA signal strength from the PRESS TE = 92 ms method is substantially larger than the GABA 3.01 ppm signal obtainable by J difference editing. A computer simulation indicated that, for a GABA-to-Cr concentration ratio of 1:8, a GABA 2.28 ppm to Cr 3.03 ppm signal amplitude ratio is 3.7% in PRESS TE = 92 ms whereas J difference editing can give a GABA 3.01 ppm signal only up to 2% of the Cr signal depending on the slice-selective RF pulse bandwidth.

Several prior 7T MRS studies reported GABA measures together with other brain metabolites, obtained with conventional MRS sequence schemes at relatively short TEs (6 and 35 ms) (10–12). The tCr concentration estimates of the present study and the prior studies are similar for medial occipital brain (8 mM *vs.* 8 – 8.7 μmol/g). For this brain region, our GABA estimate is somewhat smaller than the estimates in the prior studies (0.8 mM *vs.* 1 – 1.5 μmol/g). The GABA CRLB was quite smaller in our study (5 – 6%) compared to the prior studies (7 – 15%). For Glu, our estimate of 9.1 mM agrees well with the prior studies (9 – 10 μmol/g), with mean CRLBs ≤2% in all the studies. Gln was measured at various levels (1.5 – 3 μmol/g) in the prior studies, among which our Gln estimate of 2.3 mM is close to the measurements (2.2 – 3 μmol/g) at TE = 6 ms (10,11). Published concentrations of GSH are between 0.9 and 1.4 μmol/g while our estimation is 0.8 mM. The mean CRLBs of Gln and GSH are slightly lower in the current study (3 and 6% respectively) than in the prior studies (4 – 13%).

At 7T, while GABA may be measurable by means of uniform excitation over the entire resonances as demonstrated in the present and aforementioned prior studies (10–12), some studies measured GABA using spectral editing such as difference editing or polarization transfer methods (24–26), which edited the GABA 3.01 ppm C4-proton resonance utilizing its J coupling to the 1.9 ppm C3-proton resonance. A notable difference between the uniform excitation and spectral editing methods is homocarnosine contamination. Due to the close proximity of the homocarnosine C4 and C3 proton resonances to the free GABA C4 and C3 proton resonances, the homocarnosine C4 proton resonance will be fully co-edited in GABA editing and consequently the edited signal at ~3 ppm will be representative of the concentrations of GABA plus homocarnosine (assuming no other contamination). In contrast, the performance of a uniform excitation method may be largely dependent on the selectivity of the GABA 2.28 ppm C2-proton resonance. Generating a well-defined GABA 2.28 ppm signal against the neighboring abundant Glu signal would therefore be essential for reliable estimation of GABA. Since the homocarnosine 2.35 ppm C2-proton resonance (16,27) is relatively distant from the GABA C2-proton resonance, GABA estimation by uniform excitation may be quite immune to homocarnosine contamination. Interestingly, our GABA estimates of 0.8 – 1.0 mM in medial frontal and occipital brain are in good agreement with prior spectrally-edited free GABA estimates that were obtained with a correction for homocarnosine contamination (24,27) assuming a homocarnosine-to-free GABA concentration ratio of 1/3 (28). In biopsies from frontal, temporal and cerebellar cortices of the human brain, the homocarnosine concentration was measured to be about 50% of the free GABA level (29).

GM and WM dependence of GABA was evaluated in several prior MRS studies, mostly 3T, which all performed regression analyses to obtain the GABA levels in pure GM and WM (7,8,30,31). In the current study, the GM-to-WM GABA concentration ratio was about the same between frontal and occipital brain (~7.5). This value is in good agreement with a prior measure (~8) by spectroscopy imaging, in which the GABA 3.01 ppm was measured with double-quantum editing and a nonlinear regression was undertaken on point-spread-function corrected estimates of GABA/tCr, mostly from posterior brain (7). Our estimate for occipital-GM GABA is lower by ~30% compared to this prior study (1.0 *vs*. 1.3 mM) in which homocarnosine was likely included in GABA estimates. A similar GM-to-WM GABA concentration ratio (8.7) was obtained from a linear regression in a prior single-voxel MRS study in sensorimotor cortex (31), in which the GM GABA estimate was quite large (2.8 mM). However, the GM-to-WM GABA concentration ratio from the present study is much larger than those (2 – 3) from other prior studies (8,30). For regional variations in GABA, our observation of higher GABA in MF than in MO agrees with a recent 3T study which reported GABA levels in four regions in anterior and posterior cingulate cortices (32). In this prior study, GABA was measured to be significantly higher in anterior cingulate cortex than in posterior cingulate cortex while the fractional GM content within the voxel in the anterior region was lower than that in the posterior. In contrast, GABA was measured to be higher in posterior brain than in anterior brain in other 3T study (33). The cerebellar GABA level was measured to be lower than the anterior cingulate GABA level in another prior 3T study (34). It may be that the GABA concentration and its dependence on tissue

composition vary from one anatomical location to another and the GABA measures of the current study could be specific to the locations investigated.

Several prior spectroscopic imaging and single-voxel MRS studies evaluated Glu in GM and WM with regression analyses (35–38). The GM-to-WM ratio of Glu is in good agreement between the present and prior studies (2 – 2.5) most likely because of the relatively high concentration and consequently large signal. In contrast, there is paucity in literature for regional variations in Gln and GSH, perhaps due to the presence of technical challenges in measuring these relatively low concentration metabolites. While in our study Gln was estimated to be substantially higher in GM than in WM in frontal brain and to be about the same between GM and WM in occipital brain, a prior spectroscopic imaging study at 7T (38) showed that Gln is about 2 fold higher in GM than in WM in the supplementary motor area. Compared to a single-voxel MRS study at 7T (39), which reported metabolite ratios (/tCr) from MRS voxels (~15 mL) in medial frontal and right frontal brain (without regression), the $(Gln/tCr)_{MF}$-to-$(Gln/tCr)_{LF}$ ratio of the present study (calculated from Table 1) is quite large compared to the $(Gln/tCr)_{MF}$-to-$(Gln/tCr)_{Right\text{-}Frontal}$ ratio of the prior study (2.4 *vs*. 1.3). For GSH, the GM-to-WM concentration ratio of ~1.2 (frontal brain) in the present study is slightly smaller than a value (1.5) from a prior spectroscopic imaging study (difference editing of the GSH 2.95 ppm resonance) (40), in which the GSH level was estimated to be 3.2 and 2.2 mM for GM and WM, respectively. Our observation of higher GSH in frontal GM than in occipital GM agrees with the result from this prior study. For NAAG, our measures of the concentrations in the GM- and WM-dominant voxels (~1 and ~2 mM respectively) agree well with the reported values in prior MRS studies (10,41,42). The NAAG-to-NAA ratios in the GM and WM voxels of the present study, which were respectively ~0.1 and ~0.2 for both frontal and occipital brain, show slight discrepancy compared to some previous studies (41,43), but are in good agreement with recent 3T and 7T studies (44,45).

Several weaknesses and sources of errors may be present in the present study. First, while spectral simplification by the use of a relatively long TE (92 ms) may be beneficial, quantification of metabolite levels requires correction for T_2 relaxation effects. Since the T_2 effects in GABA, Gln and GSH were corrected using the Glu T_2 value, uncertainties may be present in the estimation of GABA, Gln and GSH, depending on the differences in their T_2's from the Glu T_2. Second, slice displacements due to the limited bandwidth of the 180° RF pulse were quite large (~10% of the slice thickness per 0.5 ppm), preventing estimation of metabolites in an identical volume. Third, although the NAA CH_2 multiplet at ~2.5 ppm was substantially suppressed with PRESS TE = 92 ms, the residual signal was not negligible compared to the C4-proton multiplets of Gln and GSH and thus could interfere with estimation of these metabolites. It appears that the NAA multiplet at ~2.5 ppm can be further suppressed by applying an additional RF pulse between the PRESS 180° pulses (39), although this may require additional echo time optimization. In the present study, a short-TE (13 ms) STEAM water signal was obtained from a single voxel and used for metabolite estimation. As shown in Table 1, the fractional GM contents within the NAA 2.01 ppm and tCho 3.21 ppm resonance voxels in left frontal brain differed by ~7% from that of the ~2.5 ppm resonance voxel. It is expected however that, with published water concentrations in

GM and WM (81% and 71% relative to the bulk water concentration respectively (46)), the GM+WM water signals from the shifted voxels may differ by ~1% from the acquired water signal. This is within the experimental errors *in vivo*. Also, errors could be introduced due to the difference in the slice profiles of the STEAM 90° and PRESS 180° RF pulses, whose ratios of the transition width to the bandwidth at half amplitude were 10% and 12% respectively. The discrepancy between the STEAM and PRESS voxel shapes was ignored in this study. Lastly, presence of potential residual MM signals near 2.28 ppm could influence estimation of GABA by the proposed method. Although the MM resonance at ~2.3 ppm may undergo very rapid T_2 relaxation (*i.e.*, ~10 fold faster compared to the Cr CH_3 resonance (47)) and consequently the signals are extensively attenuated at TE = 92 ms at 7T, precise evaluation of the MM 2.3 ppm multiplet resonance (13) would be required for ensuring GABA detection without MM interferences. However, it is likely that, given similar MM concentrations between GM and WM regions (8), the notable difference in the 2.28 ppm signal strengths in our spectra from medial frontal and left frontal voxels (see Fig. 3) may be primarily due to the regional difference in GABA, implying that our GABA estimates may not contain substantial MM contaminations.

In conclusion, we have measured GABA and other challenging metabolites in several regions in healthy human brain, using a GABA-optimized PRESS method at 7T *in vivo*. Linear regression of the GABA estimates with respect to the fractional GM content indicated that GABA is 7 – 8 fold higher in GM than in WM. The concentrations of Glu and tCr were about 2 fold higher in GM than in WM while NAAG was notably higher in WM than in GM. The dependence of Gln and tCho on tissue composition was markedly different between frontal and occipital brain. These results suggest that evaluation of potential alterations in the metabolites in disease conditions may require comparison of the estimates from matched brain regions and/or interpretation of the metabolite measures together with the tissue contents.

Acknowledgments

This work was supported by US National Institute of Health grants MH093959 and CA159128, and by Cancer Prevention Research Institute of Texas grants RP140021-P04 and RP130427. We thank Dr. Ivan Dimitrov for technical assistance.

Abbreviations used

CRLB	Cramer-Rao lower bounds
FWHM	full width at half magnitude
GABA	γ-aminobutyric acid
Gln	glutamine
Glu	glutamate
Gly	glycine
GM	gray matter
GSH	glutathione

Lac	lactate
LF	left frontal
LO	left occipital
MM	macromolecule
MF	medial frontal
MO	medial occipital
NAA	N-acetylaspartate
NAAG	N-acetylaspartylglutamate
NSA	number of signal averages
PRESS	point resolved spectroscopy
RF	radio frequency
SNR	signal-to-noise ratio
STEAM	stimulated echo acquisition mode
tCho	total choline (glycerophosphocholine + phosphoryl choline)
tCr	total creatine (creatine + phosphocreatine)
WM	white matter

References

1. Barker, PB.; Bizzi, A.; De Stefano, N.; Gullapalli, RP.; Lin, DDM. Clinical MR Spectroscopy: Techniques and Applications. Cambridge: Cambridge University Press; 2010.
2. Govindaraju V, Young K, Maudsley AA. Proton NMR chemical shifts and coupling constants for brain metabolites. NMR Biomed. 2000; 13:129–153. [PubMed: 10861994]
3. Rothman DL, Petroff OA, Behar KL, Mattson RH. Localized ^{1}H NMR measurements of gamma-aminobutyric acid in human brain in vivo. Proc Natl Acad Sci USA. 1993; 90:5662–5666. [PubMed: 8516315]
4. Mescher M, Merkle H, Kirsch J, Garwood M, Gruetter R. Simultaneous in vivo spectral editing and water suppression. NMR Biomed. 1998; 11:266–272. [PubMed: 9802468]
5. Kaiser LG, Young K, Meyerhoff DJ, Mueller SG, Matson GB. A detailed analysis of localized J-difference GABA editing: theoretical and experimental study at 4 T. NMR Biomed. 2008; 21:22–32. [PubMed: 17377933]
6. Mullins PG, McGonigle DJ, O'Gorman RL, Puts NA, Vidyasagar R, Evans CJ, Edden RA. Cardiff Symposium on MRSoG. Current practice in the use of MEGA-PRESS spectroscopy for the detection of GABA. NeuroImage. 2014; 86:43–52. [PubMed: 23246994]
7. Choi IY, Lee SP, Merkle H, Shen J. In vivo detection of gray and white matter differences in GABA concentration in the human brain. NeuroImage. 2006; 33:85–93. [PubMed: 16884929]
8. Choi C, Bhardwaj PP, Kalra S, Casault CA, Yasmin US, Allen PS, Coupland NJ. Measurement of GABA and contaminants in gray and white matter in human brain in vivo. Magn Reson Med. 2007; 58:27–33. [PubMed: 17659613]
9. Tkac I, Andersen P, Adriany G, Merkle H, Ugurbil K, Gruetter R. In vivo ^{1}H NMR spectroscopy of the human brain at 7 T. Magn Reson Med. 2001; 46:451–456. [PubMed: 11550235]

10. Tkac I, Oz G, Adriany G, Ugurbil K, Gruetter R. In vivo 1H NMR spectroscopy of the human brain at high magnetic fields: metabolite quantification at 4T vs. 7T. Magn Reson Med. 2009; 62:868–879. [PubMed: 19591201]
11. Mekle R, Mlynarik V, Gambarota G, Hergt M, Krueger G, Gruetter R. MR spectroscopy of the human brain with enhanced signal intensity at ultrashort echo times on a clinical platform at 3T and 7T. Magn Reson Med. 2009; 61:1279–1285. [PubMed: 19319893]
12. Marjanska M, Auerbach EJ, Valabregue R, Van de Moortele PF, Adriany G, Garwood M. Localized ^{1}H NMR spectroscopy in different regions of human brain in vivo at 7T. T_2 relaxation times and concentrations of cerebral metabolites. NMR Biomed. 2012; 25:332–339. [PubMed: 21796710]
13. Behar KL, Rothman DL, Spencer DD, Petroff OA. Analysis of macromolecule resonances in ^{1}H NMR spectra of human brain. Magn Reson Med. 1994; 32:294–302. [PubMed: 7984061]
14. Seeger U, Mader I, Nagele T, Grodd W, Lutz O, Klose U. Reliable detection of macromolecules in single-volume ^{1}H NMR spectra of the human brain. Magn Reson Med. 2001; 45:948–954. [PubMed: 11378871]
15. Kreis R, Bolliger CS. The need for updates of spin system parameters, illustrated for the case of gamma-aminobutyric acid. NMR Biomed. 2012; 25:1401–1403. [PubMed: 22585581]
16. Hanstock CC, Coupland NJ, Allen PS. GABA X2 multiplet measured pre- and post-administration of vigabatrin in human brain. Magn Reson Med. 2002; 48:617–623. [PubMed: 12353278]
17. Choi C, Ganji SK, Deberardinis RJ, Hatanpaa KJ, Rakheja D, Kovacs Z, Yang XL, Mashimo T, Raisanen JM, Marin-Valencia I, Pascual JM, Madden CJ, Mickey BE, Malloy CR, Bachoo RM, Maher EA. 2-hydroxyglutarate detection by magnetic resonance spectroscopy in IDH-mutated patients with gliomas. Nat Med. 2012; 18:624–629. [PubMed: 22281806]
18. Hall EL, Stephenson MC, Price D, Morris PG. Methodology for improved detection of low concentration metabolites in MRS: optimised combination of signals from multi-element coil arrays. Neuroimage. 2014; 86:35–42. [PubMed: 23639258]
19. Provencher SW. Estimation of metabolite concentrations from localized in vivo proton NMR spectra. Magn Reson Med. 1993; 30:672–679. [PubMed: 8139448]
20. Choi C, Dimitrov IE, Douglas D, Patela A, Kaiser LG, Amezcua CA, Maher EA. Improvement of resolution for brain coupled metabolites by optimized ^{1}H MRS at 7 T. NMR Biomed. 2010; 23:1044–1052. [PubMed: 20963800]
21. Pfeuffer J, Tkac I, Provencher SW, Gruetter R. Toward an in vivo neurochemical profile: quantification of 18 metabolites in short-echo-time ^{1}H NMR spectra of the rat brain. J Magn Reson. 1999; 141:104–120. [PubMed: 10527748]
22. Friston, KJ.; Ashburner, JT.; Kiebel, SJ.; Nichols, TE.; Penny, WD. Statistical Parametric Mapping: The Analysis of Functional Brain Images. London: Academic Press; 2006.
23. Michaeli S, Garwood M, Zhu XH, DelaBarre L, Andersen P, Adriany G, Merkle H, Ugurbil K, Chen W. Proton T_2 relaxation study of water, N-acetylaspartate, and creatine in human brain using Hahn and Carr-Purcell spin echoes at 4T and 7T. Magn Reson Med. 2002; 47:629–633. [PubMed: 11948722]
24. Terpstra M, Ugurbil K, Gruetter R. Direct in vivo measurement of human cerebral GABA concentration using MEGA-editing at 7 Tesla. Magn Reson Med. 2002; 47:1009–1012. [PubMed: 11979581]
25. Andreychenko A, Boer VO, Arteaga de Castro CS, Luijten PR, Klomp DW. Efficient spectral editing at 7 T: GABA detection with MEGA-sLASER. Magn Reson Med. 2012; 68:1018–1025. [PubMed: 22213204]
26. Pan JW, Duckrow RB, Spencer DD, Avdievich NI, Hetherington HP. Selective homonuclear polarization transfer for spectroscopic imaging of GABA at 7T. Magn Reson Med. 2013; 69:310–316. [PubMed: 22505305]
27. Choi C, Coupland NJ, Hanstock CC, Ogilvie CJ, Higgins AC, Gheorghiu D, Allen PS. Brain gamma-aminobutyric acid measurement by proton double-quantum filtering with selective J rewinding. Magn Reson Med. 2005; 54:272–279. [PubMed: 16032672]

28. Petroff OA, Hyder F, Mattson RH, Rothman DL. Topiramate increases brain GABA, homocarnosine, and pyrrolidinone in patients with epilepsy. Neurology. 1999; 52:473–478. [PubMed: 10025774]
29. Lajtha, A. Chemical and Cellular Architecture. Vol. 1. New York and London: Plenum Press; 1982. Handbook of Neurochemistry; p. 164
30. Jensen JE, de Frederick BB, Renshaw PF. Grey and white matter GABA level differences in the human brain using two-dimensional, J-resolved spectroscopic imaging. NMR Biomed. 2005; 18:570–576. [PubMed: 16273508]
31. Bhattacharyya PK, Phillips MD, Stone LA, Lowe MJ. In vivo magnetic resonance spectroscopy measurement of gray-matter and white-matter gamma-aminobutyric acid concentration in sensorimotor cortex using a motion-controlled MEGA point-resolved spectroscopy sequence. Magn Reson Imaging. 2011; 29:374–379. [PubMed: 21232891]
32. Dou W, Palomero-Gallagher N, van Tol MJ, Kaufmann J, Zhong K, Bernstein HG, Heinze HJ, Speck O, Walter M. Systematic regional variations of GABA, glutamine, and glutamate concentrations follow receptor fingerprints of human cingulate cortex. J Neurosci. 2013; 33:12698–12704. [PubMed: 23904606]
33. van der Veen JW, Shen J. Regional difference in GABA levels between medial prefrontal and occipital cortices. J Magn Reson Imaging. 2013; 38:745–750. [PubMed: 23349060]
34. Waddell KW, Zanjanipour P, Pradhan S, Xu L, Welch EB, Joers JM, Martin PR, Avison MJ, Gore JC. Anterior cingulate and cerebellar GABA and Glu correlations measured by ^{1}H J-difference spectroscopy. Magn Reson Imaging. 2011; 29:19–24. [PubMed: 20884148]
35. Choi C, Coupland NJ, Bhardwaj PP, Kalra S, Casault CA, Reid K, Allen PS. T2 measurement and quantification of glutamate in human brain in vivo. Magn Reson Med. 2006; 56:971–977. [PubMed: 17029225]
36. Srinivasan R, Cunningham C, Chen A, Vigneron D, Hurd R, Nelson S, Pelletier D. TE-averaged two-dimensional proton spectroscopic imaging of glutamate at 3 T. NeuroImage. 2006; 30:1171–1178. [PubMed: 16431138]
37. Posse S, Otazo R, Caprihan A, Bustillo J, Chen H, Henry PG, Marjanska M, Gasparovic C, Zuo C, Magnotta V, Mueller B, Mullins P, Renshaw P, Ugurbil K, Lim KO, Alger JR. Proton echo-planar spectroscopic imaging of J-coupled resonances in human brain at 3 and 4 Tesla. Magn Reson Med. 2007; 58:236–244. [PubMed: 17610279]
38. Pan JW, Avdievich N, Hetherington HP. J-refocused coherence transfer spectroscopic imaging at 7 T in human brain. Magn Reson Med. 2010; 64:1237–1246. [PubMed: 20648684]
39. An, L.; Li, S.; Murdoch, JB.; Shen, J. Detection of glutamate and glutamine by RF suppression and TE optimization at 7T. Proceedings of the 21th Annual Meeting of ISMRM; Salt Lake City, USA. 2013. p. 3984
40. Srinivasan R, Ratiney H, Hammond-Rosenbluth KE, Pelletier D, Nelson SJ. MR spectroscopic imaging of glutathione in the white and gray matter at 7 T with an application to multiple sclerosis. Magn Reson Imaging. 2010; 28:163–170. [PubMed: 19695821]
41. Pouwels PJ, Frahm J. Differential distribution of NAA and NAAG in human brain as determined by quantitative localized proton MRS. NMR Biomed. 1997; 10:73–78. [PubMed: 9267864]
42. Edden RA, Pomper MG, Barker PB. In vivo differentiation of N-acetyl aspartyl glutamate from N-acetyl aspartate at 3 Tesla. Magn Reson Med. 2007; 57:977–982. [PubMed: 17534922]
43. Choi C, Ghose S, Uh J, Patel A, Dimitrov IE, Lu H, Douglas D, Ganji S. Measurement of N-acetylaspartylglutamate in the human frontal brain by ^{1}H-MRS at 7T. Magn Reson Med. 2010; 64:1247–1251. [PubMed: 20597122]
44. Zhang Y, Li S, Marenco S, Shen J. Quantitative measurement of N-acetyl-aspartyl-glutamate at 3 T using TE-averaged PRESS spectroscopy and regularized lineshape deconvolution. Magn Reson Med. 2011; 66:307–313. [PubMed: 21656565]
45. An L, Li S, Wood ET, Reich DS, Shen J. N-acetyl-aspartyl-glutamate detection in the human brain at 7 Tesla by echo time optimization and improved Wiener filtering. Magn Reson Med. (Published online 2013). 10.1002/mrm.25007

46. Norton WT, Poduslo SE, Suzuki K. Subacute sclerosing leukoencephalitis. II. Chemical studies including abnormal myelin and an abnormal ganglioside pattern. J Neuropathol Exp Neurol. 1966; 25:582–597. [PubMed: 5922554]

47. Soher BJ, Pattany PM, Matson GB, Maudsley AA. Observation of coupled 1H metabolite resonances at long TE. Magn Reson Med. 2005; 53:1283–1287. [PubMed: 15906305]

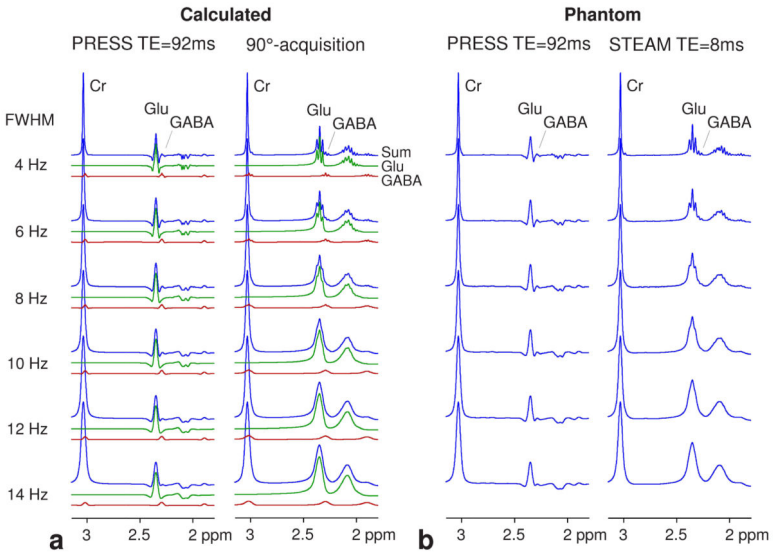

FIG 1.

Numerically-calculated and phantom spectra at 7T. (a) Spectra of GABA, Glu and Cr, calculated for PRESS (TE_1, TE_2) = (31, 61) ms and 90°-acquisition, are shown for singlet FWHM of 4 – 14 Hz. The concentration ratio is GABA:Glu:Cr = 1:10:8. (b) Spectra from a aqueous solution with GABA (2 mM), Glu (20 mM) and Cr (16 mM), obtained with PRESS TE = 92 ms and STEAM (TE, TM) = (8, 14) ms, are shown for singlet FWHM of 4 – 14 Hz. Spectra are normalized with respect to the Cr peak amplitude.

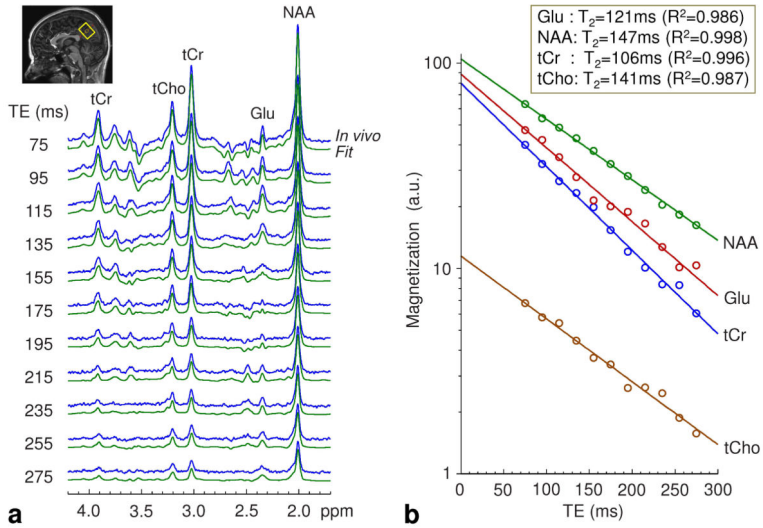

FIG 2.

T_2 measurements for Glu, NAA, tCr and tCho at 7T *in vivo*. (a) A stack of medial occipital brain spectra at 11 TEs are shown together with LCModel fits (voxel size = 23×23×23 mm^3; NSA = 32). (b) LCModel estimates of the metabolite signals at the eleven TEs were fitted with a mono-exponential function of TE. The estimated T_2 values and the coefficients of determination (R^2) are shown in a box.

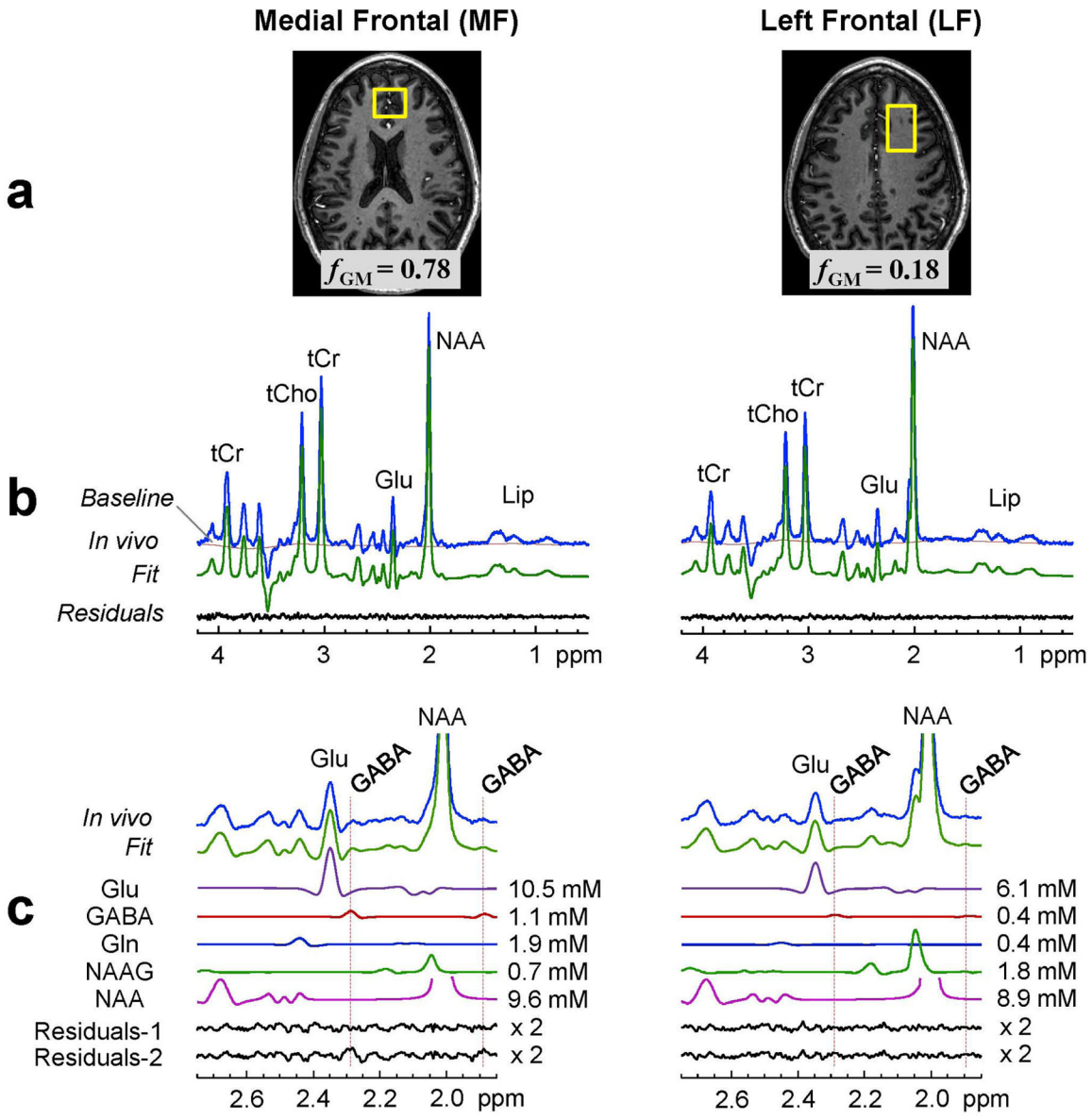

FIG 3.

Spectral analyses of *in-vivo* PRESS TE = 92 ms spectra from two brain regions. (a) Voxel positioning is shown in T_1-weighted images, together with the fractional GM contents (f_{GM}) within the voxels (size 20×23×23 and 35×20×15 mm^3 for medial frontal and left frontal brain respectively). (b) Spectra are shown with LCModel fits, residuals and baseline between 1.8 and 4.2 ppm. Data were acquired with NSA = 128 for medial frontal and 256 for left frontal. Spectra are normalized to GM+WM water. (c) *In-vivo* spectra and LCModel fits are shown between 1.85 and 2.75 ppm together with metabolite signals and concentration estimates. Residual-1 and -2 (both two-fold magnified) were obtained from spectral fittings using basis sets with and without GABA, respectively. Dotted lines are drawn at 2.28 and 1.89 ppm (GABA resonances), at which large residual signals were discernible in Residuals-2 from medial frontal.

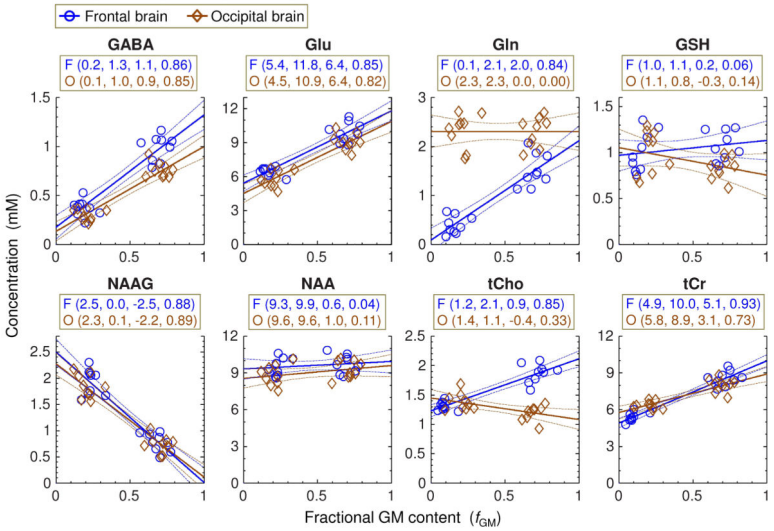

FIG 4.

Linear regression of metabolite estimates with respect to fractional GM contents (f_{GM}). The regression was performed for 8 metabolites, separately for frontal brain data (18 circles in blue) and occipital brain data (18 diamonds in brown). Shown in a bracket (within a box) for frontal (F) or occipital (O) brain is, left to right, Y-axis intercepts at f_{GM} = 0 and 1, slope, and R^2 (coefficient of determination). Dashed lines indicate 95% confidence intervals of the linear fits.

Table 1

Fractional GM contents (f_{GM}), concentration estimates (mM), and CRLB (%) are tabulated for eight metabolites for the medial frontal (MF), left frontal (LF), medial occipital (MO), and left occipital (LO) brain in nine subjects. Metabolite concentrations in the four regions were calculated with reference to the mean tCr of the MO region at 8 mM (indicated by an asterisk) following the normalization of LCModel estimates to the GM+WM water signal for individual spectra. Data are mean ± SD (n = 9).

	f_{GM} (%)				Concentration (mM)				CRLB (%)			
	MF	**LF**	**MO**	**LO**	**MF**	**LF**	**MO**	**LO**	**MF**	**LF**	**MO**	**LO**
GABA	69±6	18±5	70±6	21±6	1.0±0.1	0.4±0.1	0.8±0.1	0.3±0.1	5.1±0.6	9.8±2.6	5.4±0.9	12±2
Glu	69±6	17±5	70±6	21±6	9.9±0.9	6.5±0.4	9.1±0.7	5.8±0.7	1.1±0.3	1.6±0.5	1.3±0.5	1.6±0.5
Gln	70±6	17±5	70±6	21±6	1.5±0.3	0.4±0.2	2.3±0.3	2.3±0.3	4.7±1.2	17±7	3.1±0.3	2.7±0.5
GSH	70±7	16±5	70±6	21±6	1.1±0.2	1.0±0.2	0.8±0.1	1.0±0.2	5.0±0.7	4.8±0.7	6.0±0.7	4.7±0.9
NAAG	68±6	24±4	70±6	21±6	0.8±0.2	1.9±0.2	0.7±0.2	1.8±0.2	5.1±1.2	2.3±0.5	5.0±1.0	2.3±0.7
NAA	68±6	24±4	70±6	21±6	9.7±0.7	9.5±0.7	9.3±0.7	8.8±0.8	1	0.9±0.3	0.9±0.3	0.7±0.5
tCho	72±7	10±4	69±5	20±6	1.9±0.2	1.3±0.1	1.2±0.1	1.4±0.1	1	1	1	1
tCr	72±7	11±5	69±5	20±6	8.6±0.6	5.4±0.4	8* (±0.6)	6.4±0.3	1	1	0.9±0.3	0.6±0.5